

Project Report

On

**Development and Characterization of Al-Mg-Cu (Ni)
by Powder Metallurgy route**

By

Saksham Goel (R240211021)

Prateek Chopra (R240211040)

Under the Guidance of

Dr. Sidharth Jain

Assistant Professor (Department of Mechanical Engineering)



**B.Tech – Material Science Engineering with specialization in
Nanotechnology (2011-2015)**

College of Engineering Studies

University of Petroleum and Energy Studies, Dehradun

Certificate

We declare that we carried out the work reported in here in the Department of Mechanical Engineering, University of Petroleum and Energy Studies, under the supervision of Dr. Sidharth Jain. We solemnly declare that to the best of my/our knowledge, no part of this report has been submitted here or elsewhere in a previous application for award of a degree. All sources of knowledge used and cited have been fully acknowledged.

Saksham Goel (500017325)
Prateek Chopra (500017734)



Acknowledgement

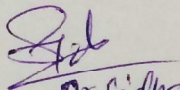
It was a great experience for us to have worked under the excellent guidance of our mentor **Dr. Sidharth Jain** (Department of Mechanical Engineering) and co-members. This major project report has not only given us an insight into the metallurgical field, but has also instilled in us a sense of team work with full utilization of the resources available.

This training would not have been possible without the indispensable support of the activity coordinator **Dr. Garimella Venkata Subrahmanyam** and other faculty members who guided us through the project. Last, but not the least, I would like to thank the lab assistant, **Mr. Anuj Rana** for their immense support during our project.



APPROVAL

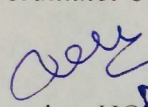
This is to certify that the project titled "Development and characterization of Al-Mg-Cu by Powder Metallurgy", carried out by Saksham Goel and Prateek Chopra has been read and approved for meeting part of the requirements and regulations governing the award of the Bachelor of Technology with specialization in Material Sciences and Nanotechnology of University of Petroleum and Energy Studies, India.


Dr. Sidhorth Jain
Supervisor/s' Name and Signature

DATE 23/4/15

Coordinator's Name and Signature

DATE


Dr. Ajay Kumar
Associate Head
Associate Head
Associate Head
Associate Head
Associate HOD/HOD's Name and Signature

DATE 23/4/15

ABSTRACT

The effort to improve automobile efficiency has potential economic and environmental advantages. The field of aluminum powder metallurgy is of specific interest as the implementation of such technologies to produce parts can offer the combination of a weight savings and the economic advantages of near net shape processing. However, one of the obstacles to overcome in the field of Powder Metallurgy is the presence of porosity in the sintered product. To decrease the presence of this property, sintered materials can be hot forged to full density. To broaden the range of applications for aluminum Powder Metallurgy technology considerable research efforts have emphasized the development of new aluminum Powder Metallurgy alloys that offer improved mechanical performance.



Table Of Contents

<u>S.No.</u>	<u>TITLE</u>	<u>PAGE NO.</u>
1	INTRODUCTION	1
1.1	General	2
2	LITERATURE REVIEW	5
2.1	Introduction	5
2.2	Powder Metallurgy of Aluminum and its alloys	6
2.3	Sintering of Aluminum	7
2.3.1	Effects of Sintering atmosphere	7
2.3.2	Effect of liquid phases on sintering densification	9
2.4	Deformation Processing of Aluminum Powder Metallurgy alloys	15
3	EXPERIMENTAL PROCEDURE	17
3.1	Introduction	18
3.2	Materials	18
3.2.1	Pure aluminum, magnesium and pre alloyed powders	18
3.2.2	Copper Nickel Powder	18
3.2.3	Balls of Ball Bearing	18
3.2.4	Lubricants for Cold Compaction Process	19
3.2.5	Hot Pressing Lubricant	19
3.2.6	Gases	19
3.3	Processing	19
3.3.1	Incorporation of Mg as a sintering aid in Aluminum powder	19
3.3.2	Incorporation of different composition of Cu-Ni in Al-0.5 wt. % Mg	20
3.3.3	Cold Compaction of the prepared samples	20
3.3.4	Sintering Process	21
3.3.5	Hot Compaction	23
3.4	Characterization	23
3.4.1	Density	23
3.4.1.1	Nominal densities of matrix alloys	23
3.4.1.2	Theoretical Composite Density	23
3.4.1.3	Density of green compacts	24
3.4.1.4	Density of sintered compacts	24
3.4.1.5	Densification Parameter	24
3.5	Microstructure	25

3.5.1	Sample Preparation	25
3.5.2	Etchants and Optical Micrography	26
4	RESULTS AND DISCUSSION	27
4.1	Introduction	28
4.2	Characterization of Sintered Specimen	28
4.2.1	Microstructure	28
4.2.1.1	Pure Al Sample	29
4.2.1.2	Al-Mg Sample	30
4.2.1.3	Al-Mg-1Cu (Ni)	31
4.2.1.4	Al-Mg-5Cu (Ni)	32
4.2.2	Density	33
4.2.2.1	Theoretical Density	33
4.2.3	Micro Hardness	34
4.2.3.1	Before Hot Pressing	34
4.2.3.2	After Hot Pressing	35
5	CONCLUSION	36
6	REFERENCES	38



List Of Figures

<u>Fig. No.</u>	<u>FIGURE TITLE</u>	<u>PAGE NO.</u>
2.1	Powder Metallurgy Process	5
2.2	Graphical representation of spinel ($MgAl_2O_4$) formation over an aluminum particle (Padmavathi and Upadhyaya, 2011)	8
2.3	Dilatometry curves for Al-xMg alloys, where x is 0, 0.15 and 1.5 wt. % Mg showing the effect of trace additions of magnesium on the sintering response of aluminum	12
2.4	Typical microstructure of a pressed and sintered material	15
3.1	Al-Mg pre alloyed powder	18
3.2	Balls of Ball Bearing	19
3.3	Alphie 3D Mixer for Blending	20
3.4	Hydraulic Pressing Machine used for Compaction	20
3.5	Schematic of Compaction Process	21
3.6	Mechanism followed during Sintering	21
3.7	Sintering Phenomena	22
3.8	Tubular Furnace for Sintering Process	23
3.9	Variable Speed Double disc polisher	25
3.10	Belt Grinder	25
3.11	Metallurgical Microscope	26
3.12	Micro-hardness Machine	26
4.1 (a)	Microstructures of pure Al at 10x, 20x, 50x, 100x before Hot Pressing	29
4.1 (b)	Microstructures of pure Al at 10x, 20x, 50x, 100x after Hot Pressing	29
4.2 (a)	Microstructures of Al-Mg at 10x, 20x, 50x, 100x before Hot Pressing	30
4.2 (b)	Microstructures of Al-Mg at 10x, 20x, 50x, 100x after Hot Pressing	30
4.3 (a)	Microstructures of Al-Mg-1 Cu (Ni) at 10x, 20x, 50x, 100x before Hot Pressing	31
4.3 (b)	Microstructures of Al-Mg-1 Cu (Ni) at 10x, 20x, 50x, 100x after Hot Pressing	31
4.4 (a)	Microstructures of Al-Mg-5 Cu (Ni) at 10x, 20x, 50x, 100x before Hot Pressing	32
4.4 (b)	Microstructures of Al-Mg-5 Cu (Ni) at 10x, 20x, 50x, 100x after Hot Pressing	32

List Of Tables

<u>Table No.</u>	<u>TABLE TITLE</u>	<u>PAGE NO.</u>
4.1	Composition of Al-Mg	33
4.2	Composition of Al-Mg-1Cu(Ni)	33
4.3	Composition of Al-Mg-5Cu (Ni)	33
4.4	Theoretical Densities of the sample	34
4.5	Micro-hardness before Hot Pressing	34
4.6	Micro-hardness after Hot Pressing	35



INTRODUCTION



CHAPTER 1

INTRODUCTION

1.1 General

The term “composite” broadly refers to a material system which is composed of a discrete constituent (the reinforcement) distributed in a continuous phase (the matrix), and which derives its distinguishing characteristics from the properties of its constituents, from the geometry and architecture of the constituents and from the properties of the boundaries (interfaces) between different constituents. Composites are materials made from two or more constituent materials with significantly different physical or chemical properties, that when combined, produce a material with characteristics different from the individual components. The individual components remain separate and distinct within the finished structure. The new material may be preferred for many reasons: common examples include materials which are stronger, lighter or less expensive when compared to traditional materials.

Composite materials are usually classified on the basis of the physical or chemical nature of the matrix phase e.g., polymer matrix, metal-matrix, ceramic-matrix, intermetallic-matrix and carbon-matrix composites. A metal matrix composite (MMC) combines a single material, a metallic base, with a reinforcing constituent, which may be metallic or non-metallic. There are several reasons why MMCs have generated considerable interest within the materials community for nearly 30 years:

- i. The “composite” approach to metallurgical processing is the only pathway for production of entire classes of metallic materials. The approach offers significant alterations in the physical properties of metallic materials like enhanced elastic moduli. Composites also offer the only pathway for producing materials with tailored physical property combinations: e.g., low thermal expansion combined with high thermal conductivity, a combination of importance for electronic packaging (Shercliff and Ashby, 1994).
- ii. MMCs offer significant improvements with regards to several properties like tolerance of high temperature, transverse strength, hardness, resistance to aggressive environments including chemicals, cryogenic or organic fluids, atomic oxygen and ultraviolet radiation, high dimensional stability, good impact, corrosion and wear resistance, reduced moisture absorption, non-flammability, while significantly outclassing ceramics in toughness and ductility (Campbell, 2006; Lindroos and Talvitie, 1995; Miracle, 2005; Surappa, 2003).

Liquid metallurgical techniques dominate the fabrication methods employed for MMC fabrication, on account of low cost and scalability. Many variants are reported, namely: stir casting (Hashim, et al., 1999), vortex casting (Clyne, 2000), infiltration (Kevorkijan, 2004) etc. Squeeze casting has been reported to overcome the many drawbacks of other competing processes (Yue & Chadwick, 1996). Powder metallurgical processing of MMCs is based on blending of the constituents, followed by either their cold consolidation or direct sintering, accomplished with or without application of pressure, followed by secondary consolidation (forging, extrusion or rolling) (Kaczmar, et al., 2000; Rosso, 2006; Torralba, et al., 2003). Aluminum Powder Metallurgy has been described as a versatile processing technique on

account of its ability to modify alloy chemistry to suit specific functions whilst producing a near-net-shape product, wherein, important operating parameters include particle size distribution, blending techniques, pressing, and sintering (Kipouros, Caley, & Bishop, 2006).

The present investigation is based on incorporation of copper particles in Powder Metallurgy aluminum matrices and their characterization. Important considerations for this work include the selection of materials, blending of the constituents, sintering of aluminum and post-sinter secondary consolidation to achieve porosity free artifacts. The developed composites will be characterized for mechanical behaviour, microstructure changes etc.

The results of the present research work have been analyzed and discussed in light of available literature to propose an insight into mechanical, thermomechanical and thermophysical characteristics of the developed of copper reinforced aluminum based Powder Metallurgy composites.

Powder Metallurgy has gained vast importance these days including the following reasons but not limiting to them:

- Certain metals that are difficult to fabricate by other methods can be shaped by powder metallurgy. Example: Tungsten filaments for incandescent lamp bulbs are made by PM.
- Certain alloy combinations and cermets made by PM cannot be produced in other ways.
- PM compares favorably to most casting processes in dimensional control.
- PM production methods can be automated for economical production.
- Controlled porosity for self lubrication or filtration uses
- Constituents that do not mix can be used to make composites, each constituent retaining its individual property.



LITERATURE REVIEW

CHAPTER 2

LITERATURE REVIEW

2.1 Introduction

Powder metallurgy is the process of blending fine powdered materials, compacting them into a desired shape or form inside a mold followed by heating of the compacted powder in a controlled atmosphere, known as sintering to facilitate the formation of bonding of the powder particles to form the final part. Thus, powder metallurgy process generally consists of four basic steps, as indicated in the figure.

The steps are as follows:

- Powder Production
- Compaction
- Sintering
- Secondary Finishing Operations

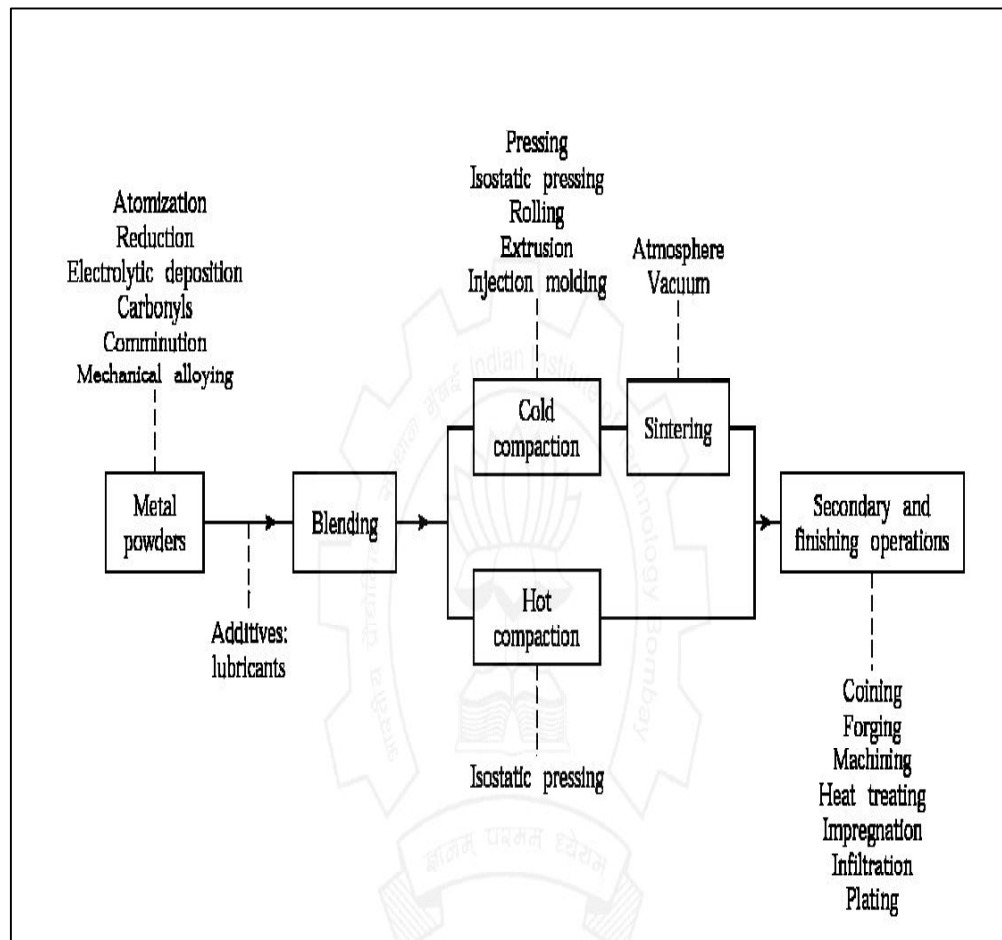


Figure 2.1: Powder Metallurgy Process

Compacting is generally performed at room temperature and at high pressure. Sintering is usually performed at elevated temperatures and at atmospheric pressure. Frequently, compacting and sintering are combined. Optional secondary processing often follows to obtain special properties or

enhanced dimensional precision. Powder Metallurgy route is very suitable for parts that are required to be manufactured from a single or multiple materials (in powder form) with very high strength and melting temperature that pose challenge for the application of casting or deformation processes.

2.2 Powder Metallurgy of Aluminum and its alloys

Pure aluminum obtained from the electrolytic reduction of alumina (Al_2O_3) is a relatively weak material. Therefore, for applications requiring greater mechanical strength, it is alloyed with metals such as copper, zinc, magnesium and manganese, usually in combinations of two or more of these elements together with iron and silicon.

Wrought aluminum alloys are divided into seven major classes according to their major alloying elements. In the internationally agreed four-digit system, the first of the four digits in the designation indicates the principal alloying element of the alloys within the group.

Aluminum alloys can be divided into two categories: heat treatable and non-heat treatable alloys. Heat treatable alloys are those in which strength is developed by precipitation hardening. Heat treatable alloys are usually found in the 2xxx (aluminum copper), 6xxx (aluminum-magnesium-silicon), and 7xxx (aluminum-zinc-magnesium) series, although a few such alloys occur in the 4xxx (copper-silicon) and 5xxx (aluminum-magnesium) series. In non-heat treatable alloys, strength is developed mainly by solid solution and by strain hardening from coldwork. The non-heat treatable alloys are in the 1xxx (aluminum), 3xxx (aluminum-manganese), 4xxx and 5xxx aluminum series, although a few such alloys occur in the 7xxx and 8xxx (aluminum-other elements) series.

The use of commercial aluminum alloys in both structural and non-structural applications has witnessed a significant expansion since the beginning of the century. Next to iron and steel, aluminum alloys are the most widely used metallic materials.

High-strength aluminum alloys of 2xxx, 6xxx and 7xxx series are used in many applications for their specific combinations of strength and corrosion resistance. In automobile and aerospace industries, the high strength-to-weight ratio of aluminum alloys (which is particularly important in the design of structural components) makes these alloys a very attractive class of materials.

Aluminum powder metallurgy has matured as a fabrication technique after the availability of almost all major alloy types. Generally prepared by inert gas atomization, a large variety of grades either completely pre-alloyed or partially pre-alloyed with elemental pre-mixes are now available to achieve component cost/weight reduction in automobiles, aerospace, electronic packaging, leisure and sport, to name a few areas of intervention (Pickens, 1981). Aluminum Powder Metallurgy offers components with equivalent mechanical and fatigue properties in comparison to wrought products of similar compositions. Lesser density for corrosion resistance, overall weight reduction, with the ability of surface modification by coatings, high thermal and electrical conductivity, particularly useful in electronic packaging and thermal management of high frequency electronic equipment, excellent machinability

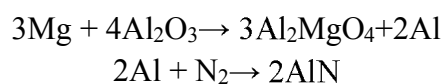
with a good response to finishing processes are some of the benefits achieved (Marketing and the Technical and Standards Committees of the Pigments and Powder Division of The Aluminum Association, 1986). Classical benefits of powder metallurgy, primarily, higher material utilization along with lower energy consumption are not only retained in aluminum Powder Metallurgy but rather amplified on account of higher strength to modulus ratio (specific strength) of finished components. Aluminum Powder Metallurgy has been labeled as a versatile processing technique on account of its ability to modify alloy chemistry to suit specific functions whilst producing a near-net-shape product, wherein, important operating parameters include particle size distribution, blending techniques, pressing, and sintering (Kipouros et al., 2006).

2.3 Sintering of Aluminum

The sintering of aluminum is difficult due to the presence of thermodynamically stable oxide shell on the particle surface, which hinders wetting and solid-state diffusion (Kondoh, et al., 2001). A dew point of less than -140°C or an oxygen partial pressure of $< 10\text{-}50$ atm. is required to reduce Al_2O_3 at standard sintering temperatures (Liu, et al., 2007; Lumley, et al., 1999; Schaffer, et al., 2005), such states are unmanageable to achieve by conventional means in either laboratory or industrial fabrication techniques, thus, a controlled atmosphere is required for sintering of aluminum. Several aspects on the role of atmosphere, powder shape and size, alloying additions, sintering aids, liquid phase fraction, sintering time and temperature have been studied. They are summarized as below, to offer an understanding on the sintering behavior of pure aluminum and alloyed powder compositions.

2.3.1 Effect of Sintering Atmosphere

In the sintering of aluminum powder based systems, the effect of atmosphere can only be studied in relation to the presence of elements that aid in disruption of oxygen from the tenacious layer of Al_2O_3 . (Pieczonka, et al., 2008) extensively studied the dilatometric shrinkage of 99% purity aluminum powder over a 600°C sintering temperature for upto 150 min duration under flowing dry $\text{N}_2\text{-H}_2$ (maximum 5 vol.% H_2), $\text{N}_2\text{-Ar}$, N_2 , Ar, and vacuum. Initial results pointed out to any visible shrinkage by N_2 only, addition of H_2 , even in small amounts reduces the shrinkage, and similar effect is observed with Ar, although at higher Ar content than H_2 . Transverse rupture strength (TRS) of N_2 sintered samples was highest, however, it was not conclusively established that nitriding of the aluminum powder, in turn, caused reduction of the Al_2O_3 and was responsible for metallurgical bonding between aluminum particles. Nitriding of the powder particles will only happen if it is preceded by reduction or rather disruption of the Al_2O_3 layer, in this case, attributed to a self-gettering mechanism due to the presence of trace additions (as impurity) of Mg in the aluminum powder. Magnesium content diffuses to the boundary of the particle and upsets the Al_2O_3 film, exposing aluminum to N_2 , as evident by the following reactions:



This is a self-replicating reaction and is generally referred to as a self-gettering mechanism, wherein oxygen is removed from the Al_2O_3 layer by forming the spinel Al_2MgO_4 and AlN . Formation of AlN , is a pre-cursor to shrinkage, and even small amounts of H_2 , inhibit AlN , thereby delaying shrinkage.

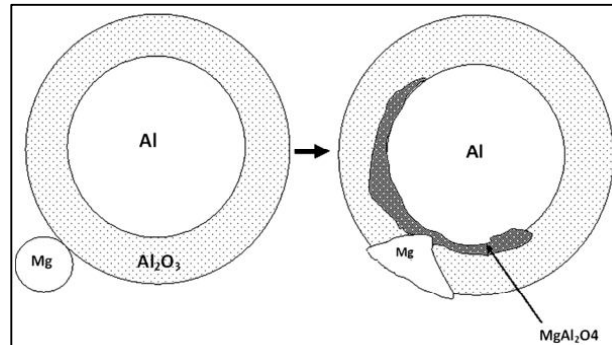


Figure 2.2: Graphical representation of spinel (MgAl_2O_4) formation over an aluminum particle (Padmavathi and Upadhyaya, 2011)

Kondoh et al., 2001, have investigated the effect of Mg on the sintering behavior and mechanical properties of Al-12Si pre-alloyed powder with elemental Sn additions under N_2 atmosphere. Presence of Sn, resulted in negligible nitration of both the pressed compacts and raw powders, leading to a persistent liquid phase that covered the particles; though, the presence of Mg helped in nitriding, even with presence of liquid Sn at the sintering temperature. Consequently, an increased intensity of metallic α -aluminum has been detected aided by Mg, through 0.0-1.0 wt.% addition. Even under the influence of Sn (upto 1.0 wt.%); Mg results in disruption of large surfaces of Al_2O_3 , incompletely wetted by liquid Sn; leading to formation of AlN . The presence of Mg, results in higher sintered densification by a factor of 2, smaller pores and a better metallurgical bond between the particles; higher elongation to failure and a dimpled fracture surface as opposed to premature brittle fracture along prior particle boundaries (PPB's) in chemistries with only Sn additions.

Densification of a green body is attained by pore closure or pore filling. (Schaffer et al., 2005) have extensively studied the role of N_2 , Ar, N_2 -5vol.% H_2 , Ar-5 vol.% H_2 (all gases with dew points below $-60^\circ\text{C} < 2$ ppm oxygen) and vacuum on the sintering characteristics of Al-Mg-Si-Cu, Al-Cu-Mg and Al-Mg-Si species of elemental powder blends. Original densification kinetics are alike for N_2 , Ar and vacuum, it is in the advanced stages of sintering that N_2 exhibits higher kinetics. This is attributed to the formation of AlN , which by itself, is not responsible for wetting of aluminum, rather Al_2O_3 has a larger contact angle, almost double in magnitude with molten aluminum, which suggests that Ar and vacuum should exhibit similar or better wettability for liquid aluminum. The release of liquid aluminum is only facilitated by spinel formation as discussed above and not by AlN . It is the formation of AlN that aids pore filling by creating a negative pressure at the pore site due to consumption of the N_2 gas at the pore site in contrast to Ar, which is non-reactive with aluminum, hence creating a back pressure and delaying pore closure. Densification in vacuum is somewhat midway N_2 and Ar. H_2 in combination with both N_2 and Ar is detrimental to densification due to formation of unstable hydrides like AlH_3 and Al_2H_6 that decompose at low temperatures, in spite of high solubility in molten aluminum, H_2 is diffused-out and further creates a back pressure at the

pore sites and inhibits pore filling. This phenomenon has not been conclusively explained but was in agreement with pore morphology. Pools of liquid fraction were found with large grain sizes at filled up pore sites. Effectiveness of sintering atmosphere for these classes of powder blends was ranked as $N_2 > \text{vacuum} > \text{Ar} > N_2 - H_2 = \text{Ar} - H_2$. The effect of N_2 on sintering characteristics of aluminum has been discussed by (Schaffer and Hall, 2002); the self-gettering mechanism of oxygen depletion and spinel formation is limited to the inner core of a green compact, through networks of interconnected pores. This is explained by the low partial pressure of oxygen deep within the green body. The outer regions, like the surface in contact with furnace wall, are largely unsintered; consequently N_2 is more effective at low green densities, wherein, large networks of continuous interconnected pores exist.

Martin and Castro, 2003, have reported enhanced sintered densification in vacuum over N_2 for 2xxx species of pre-alloyed aluminum powders at all temperatures and durations against flowing high purity N_2 ; but the higher sintered densities obtained in vacuum did not translate into better age hardening response, primarily due to the slow cooling rate achieved under vacuum against flowing N_2 , this was attributed to the amount of liquid phase present under liquid phase sintering and also the resulting morphology (shape and size) of precipitates after slow cooling.

2.3.2 Effect of liquid phases on sintering densification

In the previous section it has been seen that for sintering of aluminum powder, the oxide layer has to be disrupted or reduced. A mechanism of self-gettering seems to be the dominant player under a dry nitrogen atmosphere, as discussed above. Following this pre-requisite, there also exists a need for development of a transient or persistent liquid phase to wet over the aluminum particles and aid sintering densification. Considering these pre-conditions, it is imperative that compositions for aluminum Powder Metallurgy are developed wherein these factors are built-in.

Schaffer et al., 2001, have shown an optimum Mg content of ~0.15 wt.% causes sufficient shear stress to break up the oxide film (generally 5-15 nm thick in gas atomized powders). The role of Mg was confirmed in Al-Sn, where liquid Sn only wets Al in the presence of Mg, it seeps out otherwise (melting point of Sn 232°C). The maximum solid solubility of Sn is <0.15%, whereas Aluminum is completely soluble in liquid Sn and the diffusivity of Al in liquid Sn is about five times greater than the self diffusivity of liquid Sn (Schaffer, 2004). Sercombe and Schaffer, 1999, have stated a 20% increase in properties upon introduction of 0.1 wt.% Sn in a traditional 2xxx series alloy (Al-4.4Cu-0.8Si-0.5Mg).

Citing the work of German and co-workers, (Schaffer et al., 2001) summarized the key factors for designing an ideal liquid phase sintering system: The additive should have a lower melting point than the base, a low melting point eutectic is less beneficial as liquid fraction does not form spontaneously. The solubility of the additive in the base should be low, ensuring segregation on particle boundaries, which maximizes the liquid volume fraction. Solid solubility of the base with the additive is not an essential, but liquid solubility of the base with the liquid additive is a necessary condition. High diffusivity of the base in the additive liquid ensures high rates of mass transport and therefore rapid sintering.

Sercombe and Schaffer, 1999, have investigated the effect of trace additions of Sn, Pb, In, Bi and Sb (all <0.1 wt.%) on sintering densification of Al-4.0Cu-0.15Mg alloy. The maximum solid solubility of copper in aluminum is 5.65% at 548.2°C and the liquid phase is composed of a eutectic between Al and Al₂Cu (θ); any additive that delays the solidification of the liquid eutectic will increase the sintering densification. It was observed that even about >0.05 wt.% Sn, was sufficient to bind all the vacancies in aluminum, which reduced the diffusion of Cu into Al, whereby the liquid eutectic persisted for longer duration. Sn was ahead of Cu in the solid solution owing to its higher diffusion coefficient in aluminum. The volume of liquid phase present is the same, with Sn in trace amounts, but the duration to achieve equilibrium is longer with respect to the sintering cycle, resulting in enhanced densification. The effect is similar for other elements like Pb, Sb and Bi, which also enhance sintering densification. Addition of Ni and Zn has no effect, as they possess very weak vacancy binding energies.

MacAskill et al., 2010, studied a ternary Al-1.5Mg-1.5Sn alloy, with Mg having both a master-alloyed and an elemental presence. It was observed that Sn alone, in spite of being the liquid phase, was not able to wet the aluminum, it was only with the presence of Mg that the wetting was activated. Higher densification was achieved in alloys with elemental Mg (upto 99.5% theoretical density). Sn was instrumental in lowering the mass gain observed in sintered samples, thereby, resulting in increased sintered density, but this effect was marked in the presence of elemental Mg. This phenomenon can be attributed to higher wettability induced by Mg, wherein Sn was better able to coat the exposed aluminum particles and hinder AlN formation. Studying only the elemental source of Mg, the ductility, under tension, increased upto 1.5 wt.% Sn and decreased afterward. In the sintering response of a traditional 7xxx series Al-8Zn-2.5Mg-1Cu alloy mixed with trace additions (upto 0.16 wt.%) of Pb, Sn, Bi, Sb and Se; it was observed that, the base composition along with Sb and Bi resulted in a net expansion; Se had no effect while Sn and specifically Pb were beneficial (Schaffer and Huo, 2000). Maximum improvement in tensile strength was observed with the addition of a pre-alloyed Zn-Pb master alloy; however elemental Pb along with the master alloy negated the improvements. The mechanism behind this observation was not explained and left to further investigation. Zn is the most important element in the 7xxx series high strength alloys, primarily on account of being able to form a low temperature eutectic (380°C) with aluminum and its ability to form a persistent liquid phase for enhancing sintering densification and further improving the ageing response; but the solid solubility of Zn in aluminum makes it a non-ideal candidate as a sintering aid, even with small amounts of Pb.

The addition of Cu, however, created a net shrinkage at the sintering temperature; the benefits are attributed to improved wetting and formation of CuAl₂ intermetallic at the particle boundaries; adding up to a critical liquid volume fraction of 12%, in the present case of a supersolidus liquid phase sintering system (SLPS).

German, 1997, has stated that a SLPS occurs when a pre-alloyed powder is heated to a temperature between the solidus and liquids and the liquid phase nucleates within each particle. Densification happens by viscous flow, which starts when the fractional liquid coverage of the grain boundaries reaches 73%. This liquid phase evolving out of the pre-alloyed particles is very sensitive to heating rates (40 Kmin⁻¹ in this case with a 20 min sintering hold), wherein, slower rates leads to homogenization activated by solid-solid

solutionizing at the sintering hold. Hence, the processing parameters are equally important to ensure SLPS. In this section, only the effect of liquid phase over sintered densification and age hardening response has been covered; other process parameters will be discussed in succeeding sections.

Martin and Castro, 2003, have investigated the effect of processing parameters on liquid phase sintering (LPS) of some common pre-alloyed aluminum powder mixes corresponding to age hardenable 2xxx, 6xxx and 7xxx wrought samples. From the 2xxx pre-alloyed powder, two compositions were investigated, both showed initial swelling due to presence of a liquid phase, which helped in further densification during later stages of sintering. Higher sintering temperatures for the 6xxx alloy resulted in better final density, because of larger liquid fraction which helped in progressive densification; however, the age hardening response under T4 (natural ageing) did not significantly differ for the two sintering temperatures, indicating grain coarsening, whereby benefits out of higher density did not translate into higher hardness; hardening phases namely Al_2Cu , Mg_2Si and MgZn_2 were detected for the three alloys respectively, in the as sintered state.

An oxide layer always covers aluminum. The thickness of the oxide is dependent on the temperature at which it formed and the atmosphere in which it is kept, particularly the humidity. The thickness on atomized powder can vary from 5-15 nm. The oxide stops solid state sintering in low melting point metals, including aluminum. This has been explained in terms of the relative diffusion rates through the oxide and the metal, for metals with stable oxides. The use of liquid phases is an alternative to solid state sintering. An essential requirement for effective liquid phase sintering is a wetting liquid. High melting point, materials such as metal oxides are generally poorly wetted by liquid metals, except at high temperatures. It is therefore apparent that the oxide on aluminum is a sintering barrier and needs to be disrupted or removed. For aluminum at 600°C , a $\text{PO}^2 < 10^{-50}$ atmospheres is required to reduce the oxide. This corresponds to a dew point of $\leq -140^\circ\text{C}$. This is impossible to obtain in conventional atmospheres. Although the oxide cannot be removed, sintering in the presence of magnesium may disrupt it. Magnesia has a lower free energy of formation than alumina and magnesium metal can partially reduce alumina to form spinel, MgAl_2O_4 . During sintering, reaction of Mg with the Al_2O_3 film breaks the oxide, which exposes the underlying metal and facilitates sintering.

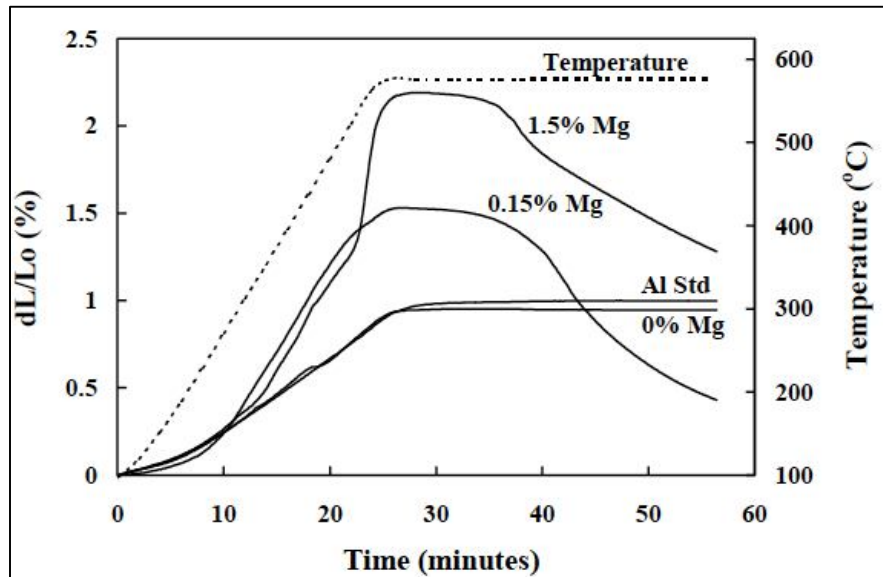


Figure 2.3: Dilatometry curves for Al-xMg alloys, where x is 0, 0.15 and 1.5 wt % Mg showing the effect of trace additions of magnesium on the sintering response of aluminum.

Based on understanding of fundamental liquid phase sintering phenomena, German recognized that it is possible to define certain ideal phase diagram characteristics. The key features of an ideal liquid phase sintering system are:

- The additive should have a lower melting point than the base. The alternate is a low melting point eutectic, which is less beneficial because liquid formation does not occur spontaneously on heating.
- The solubility of the additive in the base should be low because this ensures that the additive remains segregated to particle boundaries and maximizes the liquid volume.
- While the base should be soluble in the liquid, it is not necessary for the base to be soluble in the solid additive. Completely miscible liquids ensure that mass transport is not constrained.
- In addition, the base should also have a high diffusivity in the liquid. This ensures high rates of mass transport and therefore rapid sintering.

Delgado et al., 2005, have investigated the addition of Al-12Si (eutectic) pre-alloyed powder to pre-alloyed as well as elemental AA2014 as a sintering aid. The mechanism described here was reduction in the contact angle of the liquid phase with the aluminum particle, thereby, increasing the time for Al_2Cu (θ) to stay in the liquid phase, which forms at 548°C . This aluminum-copper eutectic is transient in nature and in low Cu levels may be completely absorbed into α -aluminum. The Al-Si eutectic forms at a higher temperature, 578°C . Increased densification along with improved mechanical properties was observed at sintering temperatures in the $580\text{--}620^\circ\text{C}$ range, with the addition of Al-12Si. Hence, increased wetting of the low temperature Al-Cu eutectic can be aided by introduction of another liquid phase, with reduced contact angle; will ensure delayed absorption into α -aluminum, increasing the duration of transient aspect and hence improved densification.

Bishop et al., 2000, have reported significant improvements in mechanical properties by trace additions of Ag-3.0 wt.% and Sn-2.0 wt.% in an inert gas atomized Al-4.4Cu-0.8Si-0.8Mn-0.5Mg (AA2014) pre-alloyed powder. SnO_2 and AgNO_3 were the sources for Sn and Ag respectively. Sn supports the formation of Al_2Cu (θ) type of precipitates in Al-Cu systems; Ag

helps in rearrangement of the θ' precipitates along a different habit plane ($\{111\}$ instead of $\{100\}$) (Ω) with a hexagonal morphology instead of tetragonal. Aluminum, being a FCC material, deforms by slip along close packed $\{111\}$ planes. Since Ω forms on the same family of planes it offers a more direct obstacle to dislocation motion than θ' , thereby resulting in improvements in mechanical properties. However, the supersolidus temperature of sintering allowed higher liquid fraction of Sn, exacerbated by longer sintering cycle time (16 hours), resulted in a Sn localization on grain boundaries and formation of a Sn-Al composite (authors claim to be useful in wear resistant applications). Ag did alter the morphology of θ' and resulted in increased strength, but no significant gains were reported in corrosion resistance.

The general sequence of precipitate ageing after a solutionizing and quench treatment in 7xxx can be expressed as: Supersaturated solid solution \rightarrow Guinier-Preston zones (GPZ) \rightarrow η' (MgZn_2) \rightarrow η (MgZn_2) (Chinh et al., 2004). It is generally accepted in Powder Metallurgy aluminum based systems for age hardenable alloys that compacts in the sintered state are considered as T1 temper; in solutionized and naturally aged condition as T4 aged and if subject to artificial ageing treatment, in T6 aged condition. The 7xxx class of alloys is known for high strength due to maximum ageing response amongst all age hardenable alloys. Similar performance is expected in Powder Metallurgy on account of high solubility of Zn in the aluminum matrix; Cu improves the wetting behavior and Mg, even in low concentrations, facilitates oxide film break-up and enhances sintering densification by self diffusion of aluminum across particle boundaries (Eksi et al., 2004). Chinh et al., 2004, have investigated the effect of Cu on the mechanical properties of Al-Zn-Mg alloys in the IM (ingot metallurgy) system and have reported that addition of Cu facilitates smoother transition from GP zones to η' , thereby retarding the rate of hardening in the early stages of natural ageing. Cu also alters the precipitate morphology from largely spherical to a mix of spherical and ellipsoidal; the spherical precipitates are free from Cu, largely composed of MgZn_2 , the ellipsoidal shape is a result of strained interface, responsible for strength enhancement.

The hardness achieved by the Powder Metallurgy alloy was equivalent to that of wrought 7075 in T6 treated condition. Calorimetric studies on the precipitation behavior showed that that followed the η (MgZn_2) based sequence typical of 7XXX series wrought alloys. In the T-6 condition, GP zones were the dominant strengthening precipitates. Elevated temperature exposure to tensile specimens of the alloy showed visible reduction in tensile strengths at temperatures corresponding to dissolution of η/η' . The effect was more pronounced in T-6 treated specimens. Fatigue life was compared with a similar wrought alloy and statistically shown to be within a 50% probability of failure; this was largely attributed to residual porosity (~ 1 vol.%), which acts as a stress raiser, thereby increasing fatigue crack sensitivity of the Powder Metallurgy alloy.

Mohammadi et al., 2010; Shahmohammadi et al., 2007, have investigated the phase evolution in elementally prepared Al-5.6Zn, Al-5.6Zn-2.5Mg and Al-5.6Zn-2.5Mg-1.6Cu wt.% powder mixes. In the Al-Zn powder mix, an expansion was recorded at 420°C, corresponding to bulk melting of Zn; this liquid phase was transient in nature owing to excessive dissolution of Zn in aluminum at this temperature; however, this liquid phase aided in a net densification at the sintering temperature (600°C). Influence of Mg to the Al-Zn powder mix aided net densification after an initial dilatation due to melting of Zn by formation of an intermetallic

eutectic between $Mg_{17}Al_{12}$ and Mg; further heating to the sintering temperature resulted in ternary intermetallic of Al-Zn-Mg. Densification was aided by presence of these intermetallic and pore filling effects due to capillarity and particle rearrangement. For the Al-Zn-Mg-Cu compacts, initial swelling was even more pronounced, but densification was aided at the sintering temperature by formation of Al-Cu eutectic in liquid phase (Schaffer et al., 2001). The effect of reduced porosity, aided by LPS, has a direct bearing on the mechanical properties of the alloy system investigated. The addition of Mg and Cu to the Al-Zn alloy has a strengthening effect by precipitation hardening; this effect is even more amplified by reduced porosity levels. Increasing the Zn and incorporation of Al-Mg master alloy powder particles is reported to give better strength and overall ageing response.

Showaiter and Youseffi, 2008, investigated the sintering behavior of Al-1.0Mg-0.6Si-0.25Cu (corresponding to wrought 6061) using elemental powders with additions of 0.12 Pb, 0.1 Sn or 0.4 Ag wt.% as sintering aids. Sintered densities were higher for the same compaction pressure and sintering temperature under N_2 , in comparison to vacuum. Amongst the sintering aids employed, addition of 0.12 wt.% Pb was most effective (almost 100% theoretical density was achieved); Sn and Ag additions did result in enhanced densification but to a lesser degree. EDX (energy dispersive x-ray) analysis of intermetallic precipitates revealed the presence of Al-Mg₂Al₃-Mg₂Si (450°C) and Al-Si-Mg₂Si (555°C) phases; further signifying the dominance of Mg₂Si as the strengthening precipitate. Localized large sized pores were visible in specimens without any sintering aids due to formation of a transient liquid phase, which on slow furnace cooling and homogenizing generated a net expansion and growth of pre-existing pores owing to Kirkendall effect. The addition of Pb, Sn and Ag has been shown to reduce the surface tension and facilitate the wetting of supersolidus liquid phase over the aluminum particles (German, 1997); however it is widely reported that the solidified liquid phase, rich in low melting point constituents as either intermetallic or eutectics, will be detrimental to mechanical properties by inducing brittleness and premature failure.

Youseffi et al., 2006, have shown from thermodynamic analysis of pre-alloyed 6061 compacts the formation of a persistent liquid phase (sintering temperature 620°C, 1hour sintering hold, N_2 atmosphere) owing to incipient melting of the powder. Intermetallic phases detected were Mg₂Si+Mg₅Al₈ (449°C); Mg₅Al₈ (450°C) and Mg₂Si (595°C). As reported earlier by the same workers, for elemental powders of same alloy composition, the dominant sintering mechanism was transient liquid phase sintering, whereas with pre-alloyed powder, sintering progressed under a persistent supersolidus liquid phase.

Sercombe, 2003, has shown that elemental additions of Mg (instrumental in disruption of tenacious oxide layer over aluminum particles) and Sn/Pb (generation of a persistent liquid phase) is most effective in sintered densification of uncompact (loose) pre-alloyed 2124 and 6061 powders, the research was conducted as a simulated experimentation of SLS (selective laser sintering); wherein layer-wise deposited polymer blended loose powder feedstock is sintered by a laser beam as the energy source. The presence of a liquid phase, at sintering temperatures (610°C for 2124 and 635°C for 6061) ensuring about 20 vol.% of liquid fraction, aided densification, further activated by the presence of elemental Mg 0.1 wt.% of Sn was sufficient for 6061 whereas 0.5 wt.% was required for 2124.

Schaffer, 2004, have summarized that aluminum Powder Metallurgy is seeing an increased interest beyond current applications areas limited by fatigue and stress applications, in marine, hand tools, office machinery and like. However, with judicious understanding of sintering mechanisms, near-net-shape, fully dense components can be realized without resorting to expensive pre-alloyed powders and capital intensive secondary thermo-mechanical processing. Such alloy design for aluminum Powder Metallurgy and composites will open new application areas driven by automotive and aerospace, harnessing, light weight, high compressibility, low sintering temperatures, easy machinability and good corrosion resistance to the advantages offered by existing Powder Metallurgy technologies.

2.4 Deformation Processing of Aluminum Powder Metallurgy Alloys

Thermo-mechanical deformation processing by forging, hot pressing, extrusion or rolling of powder (compacts) in encapsulated-vacuum de-gassed; cold pressed or sintered states have been widely reported in literature as industrially acceptable techniques to enhance the mechanical properties of components for demanding applications (Kuhn, 1978). Increments in strength, impact energy and fatigue resistance have been attributed to reduction in porosity, combined with better metallurgical bonding between particles on account of shear induced rupture of oxide film (Abdel-Rahman and El-Sheikh, 1995; Upadhyaya, 1997). Evolution of a typical material microstructure after press and sinter of aluminum based powders has been shown. It is largely composed of retained prior particle boundaries (PPB's) and sub-particle grains, rearranged particles, free standing or interconnected pores and an intermittent oxide layer.

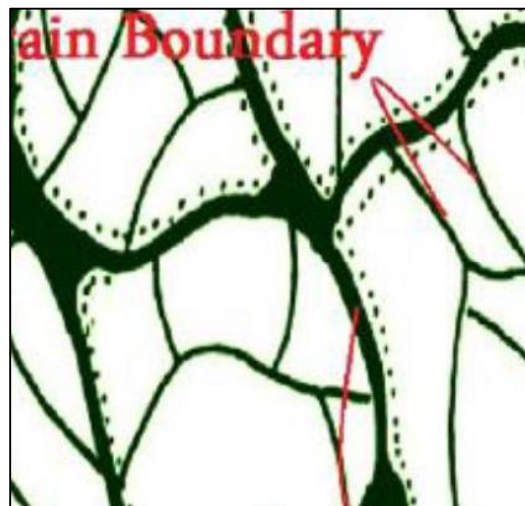


Figure 2.4: Typical microstructure of a pressed and sintered material
(Mazahery and Shabani, 2012)

To achieve optimum properties in aluminum based powder alloys, (Greasley and Shi, 1993) have outlined important stages prevalent during deformation based consolidation, as: (1) homogenization of as-rapidly solidified sub-structure of particles, leading to uniform dissolution of alloying elements, dispersoids, precipitates and phases (2) disruption of nascent oxide layer (3) creation of precipitate free zones due to high diffusion rates over free surfaces and excessive plastic work (4) effect of local strain fields that influence recovery, recrystallization and grain growth (5) upper bounds of hot working temperature and strain rate

to avoid incipient melting and hot shortness. By hot plain strain compression testing of sinter-extruded AA2014 pre-alloyed powder compacts over a range of temperatures, strain rates and imposed strain, (Greasley and Shi, 1993), have reported that strains of 0.8, (extrusion ratios of 2.5:1), are insufficient to dissolve PPB's. Strains of 1.6 (extrusion ratio 5:1) are sufficient to remove PPB's at deformation temperature $\geq 0.7 T_m$. Strains of 2.4 (extrusion ratio 11:1) are sufficient to remove PPB's at all deformation temperatures. At strains ≥ 2.4 and strain rates $\geq 6.9 \text{ s}^{-1}$, stable microstructures are attained at all working temperatures. The upper limit for extrusion temperatures to avoid incipient melting and onset of hot shortness is about 70 K lower than that determined by thermodynamic analysis for that alloy, due to frictional heat at the billet-die contact surface.



EXPERIMENTAL PROCEDURE



CHAPTER-3

EXPERIMENTAL PROCEDURE

3.1 Introduction

The powder metallurgical processing of aluminum composites requires similar equipment and processing methodology as used in classical powder metallurgy, incorporating the steps of powder chemistry preparation, cold consolidation, sintering under controlled atmosphere and if required, secondary operations on the sintered body. In the introduction of powders, for fabrication of composites, a blending step is added in the beginning to enable uniform reinforcement distribution in the matrix without altering the respective morphologies. Initial characterization starts from density measurements of green, sintered and secondary formed samples. This chapter will describe in detail about the starting materials, fabrication processes and characterization tools employed over the various stages of development of aluminum/aluminum alloy powder metallurgical (P/M) composites.

3.2 Materials

3.2.1 Pure aluminum, magnesium and pre-alloyed aluminum powders

Aluminum powder of size $95\ \mu\text{m}$ was obtained which was then mixed with Mg powder using a Alphie 3D Mixer.

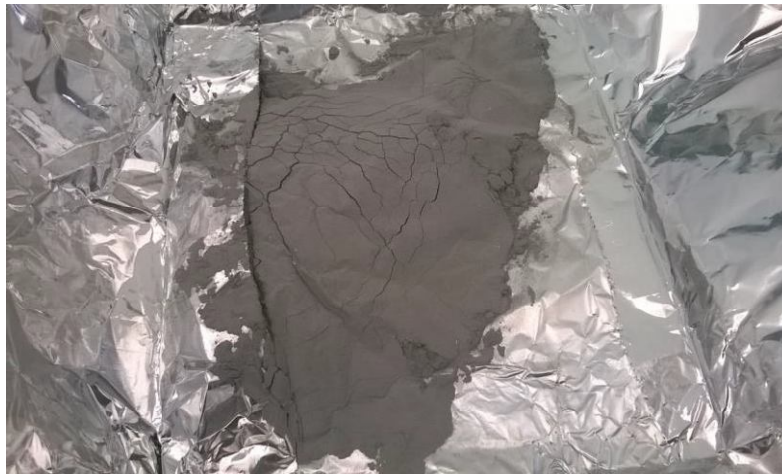


Figure 3.1: Al-Mg pre alloyed powder

3.2.2 Copper-Nickel Powder

Copper-Nickel powder was also used and was obtained from Cu-Ni brazing rods, which were of the size of $45\ \mu\text{m}$. The addition of Cu-Ni powder increased the strength to weight ratio of the mixed powder since the base element (Aluminum) used is a soft metal.

3.2.3 Balls of Ball Bearing

Balls of Ball Bearing were used in the Alphie 3D Mixer for better mixing of the powders with each other. The diameter of the balls was 8mm, 16mm, 32mm and were made of stainless

steel. This was done since there was a large difference in the compositions of the powders taken and to allow uniform mixing of the powders with each other.



Figure 3.2: Balls of Ball Bearing

3.2.4 Lubricant for Cold Compaction Process

Stearic Acid ($\text{CH}_3(\text{CH}_2)_{16}\text{CO}_2\text{H}$) flakes were dissolved in acetone and heated upto 50°C followed by continuous stirring in a magnetic stirrer. A clear liquid resulting after complete dissolution of stearic acid was used as die wall/punch-plug face lubricant during cold consolidation of matrix powders and composite powder-fiber blends.

3.2.5 Hot Pressing Lubricant

Graphite paste was used as a lubricant as well as to protect the surface of the sample from being damaged during the process of Hot Pressing. Graphite paste was also applied on the walls of the cavities for efficient pressing process.

3.2.6 Gases

Nitrogen gas (Purity > 99.99%) was used during the process of sintering so that there is decrease in the pore size in the sample by the formation of Aluminum Nitride (AlN).

3.3 Processing

3.3.1 Incorporation of Magnesium as a sintering aid in pure aluminum powder

Pure Magnesium powder and pure aluminum powder, weighed to an accuracy of 100 grams, were ball milled in a Alphi 3D Mixer to produce Al-0.5 wt. % Mg matrix powder blend. The motion of this machine is based on the “Kinematic Inversion Principle”. This unusual, 3-dimensional mixing motion quickly and efficiently produced a homogeneous substance regardless of specific weight of the substances being mixed. This makes it an ideal powder blender or liquid mixer. The speed of the mixer was maintained at 200 rpm for duration of 40 minutes. This sample was then subjected to Cold Compaction.

3.3.2 Incorporation of different composition of Copper-Nickel in the Al-0.5 wt. % Mg

Cu(Ni) powder of the size of 45 μm were taken in different compositions i.e. in 1 wt. % and 5 wt. %, were mixed with Al-0.5 wt. % Mg. Thus we obtained two samples of composition Al- 0.5 wt. % Mg- 1 wt. % Cu(Ni) and Al- 0.5 wt. % Mg- 5 wt. % Cu(Ni). The motion of this machine is based on the “Kinematic Inversion Principle”. This unusual, 3-dimensional mixing motion quickly and efficiently produced a homogeneous substance regardless of specific weight of the substances being mixed. This makes it an ideal powder blender or liquid mixer. The speed of the mixer was maintained at 200 rpm for duration of 40 minutes. These two samples were then subjected to Cold Compaction.



Figure 3.3: Alphie 3D Mixer for Blending

3.3.3 Cold Compaction of the prepared samples

Cold compaction is the process of compacting metal powder in a die through the application of high pressure. Typically the tools are held in the vertical orientation with punch tool forming the bottom cavity. The powder is then compacted into a shape and then ejected from the die cavity. The density of the compacted powder is directly proportional to the amount of pressure applied.



Figure 3.4: Hydraulic Pressing Machine used for Cold Compaction

Composite powder blends, in weighed batches were compacted in steel dies using a hydraulic pressing machine of 100T capacity (Peeco Hydraulics, Kolkata); the load was maintained at value; the press was equipped with a pressure regulating valve which was capable of delivering a dwell at maximum load. The compaction tool consisted of rectangular dies (75mm x 13mm) and circular dies (diameter= 40mm). Compaction stress was taken in terms of MPa; consequently, press tonnage in tonne (T) was set as the product of compaction stress (MPa) with projected area of the die cavity (mm²). The height of the green briquettes thus formed was dependent on the amount of filling and compaction pressure. Dies were cleaned with acetone followed by application of lubricant on die walls and punch faces prior to loading. Dies were lightly tapped after filling to obtain charge packing upto apparent density with a flat meniscus.

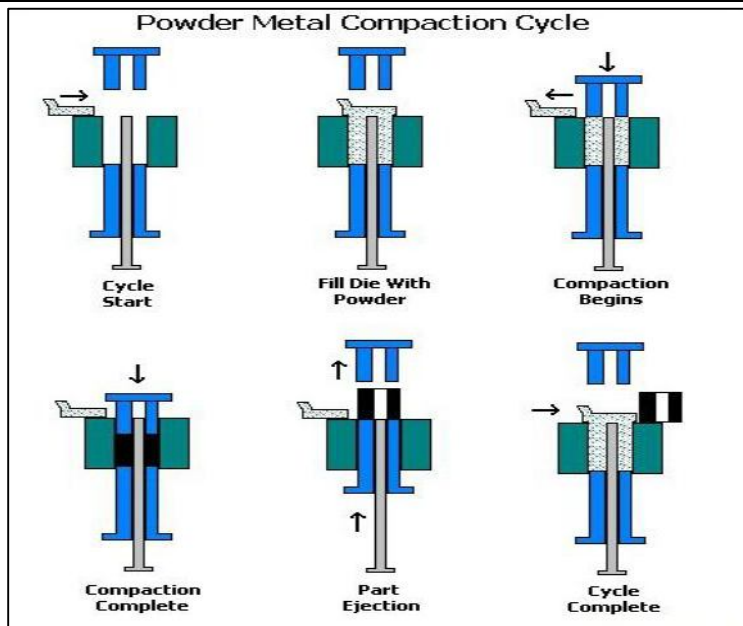


Figure 3.5: Schematic of Compaction Process

3.3.4 Sintering Process

Sintering is a heat treatment applied to a powder compact in order to impart strength and integrity to the material. The temperature used for sintering is below the melting point of the major constituent of the Powder Metallurgy material. After compaction, neighboring powder particles are held together by cold welds, which give the compact sufficient “green strength” to be handled. At sintering temperature, diffusion causes necks to form and grow at these contact points.

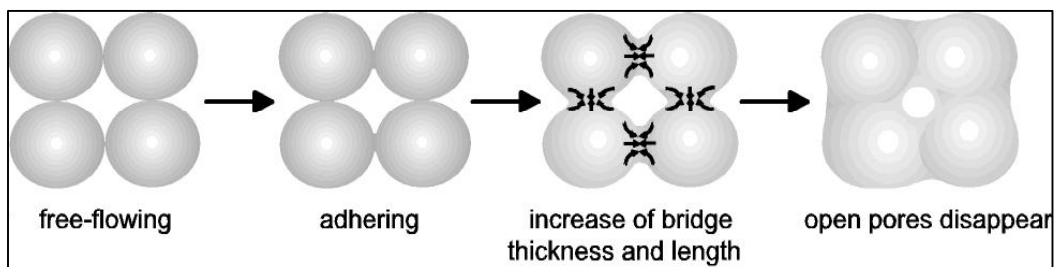


Figure 3.6: Mechanism followed during Sintering

Sintering can be considered to proceed in three stages:

- During the first, neck growth proceeds rapidly but powder particles remain discrete.
- During the second, most densification occurs, the structure recrystallizes and particles diffuse into each other.
- During the third, isolated pores tend to become spheroidal and densification continues at a much lower rate.

Composite green compacts were sintered using a self-assembled tubular furnace having a tube of 75 mm outer diameter and 1 m length. The tube was fitted with custom machined end caps stainless steel, having ball valve controlled ports for gas inlet, vacuum pump and tube pressure readout gauge. The hot zone of the furnace was 200 mm in length, extending 100 mm from the geometric center of the tube on either side, as verified by calibration against a standard

thermocouple. A typical sintering cycle, as shown in the figure, consisted of loading the green compact in the furnace hot zone, sealing of end caps, evacuation of the tube by a mono-block vacuum pump, (1) ramp-up to the degassing temperature, (2) holding at the de-gassing temperature, introduction of technical grade nitrogen in the tube, re-evacuation and back-filling of nitrogen (3-4 times), filling-up and constant flow of the gas at a desired flow rate, (3) ramp-up to the sintering temperature, (4) dwell at the sintering hold and finally (5) shutdown of power to enable furnace cooling of samples to room temperature.

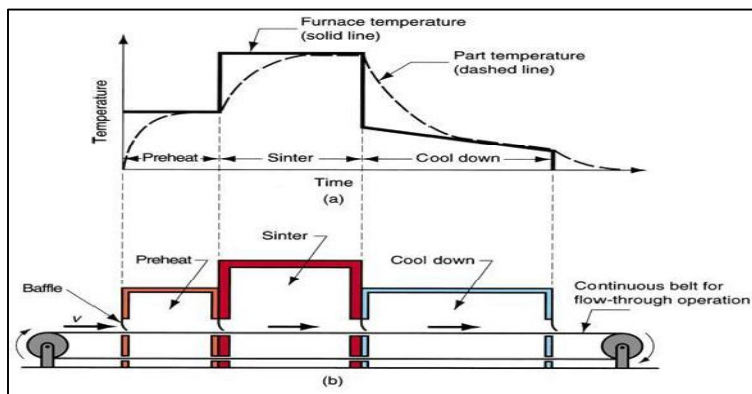


Figure 3.7: Sintering Phenomena

The furnace was heated to a temperature of 250°C for a period of 10 minutes. The samples in the furnace were held at this temperature for a period of 15 minutes. Now the temperature of the furnace was raised to 620°C over a time period of 30 minutes. After achieving the desired temperature of 620°C, the furnace was held at this temperature for 40 minutes. Now the furnace was allowed to air quench overnight. During the entire process, there was occasional flushing of Nitrogen (N_2) gas since it produces good sintered properties. Nitrogen is the only atmosphere producing excessive shrinkage compared to Argon or vacuum. When Nitrogen (N_2) gas comes in contact with the aluminum sample, it forms Aluminum Nitride (AlN) which then goes into the pore spaces and closes the pores. The formation of AlN is thought to reduce the pressure in the closed pore spaces, which unbalances the meniscus forces, inducing pore filling. Pore filling is thus an important densifying mechanism in the sintering of aluminum.



Figure 3.8: Tubular Furnace for Sintering process

3.3.5 Hot Compaction

3.4 Characterization

3.4.1 Density

3.4.1.1 Nominal densities of matrix alloys

The inverse rule of mixtures was used to calculate the nominal theoretical densities (ρ_m) of the matrix alloy by converting the given chemical composition in (mass) weight (%) fraction to volume (%) fractions and adding the respective volume fractions of the constituents, using the formula:

$$\rho_m = \frac{100}{\left(\frac{M_1}{\rho_1}\right) + \left(\frac{M_2}{\rho_2}\right) + \left(\frac{M_3}{\rho_3}\right) + \dots + \left(\frac{M_x}{\rho_x}\right)}$$

where ($M_1, M_2, M_3 \dots M_x$) and ($\rho_1, \rho_2, \rho_3 \dots \rho_x$) represent (mass) weight fractions and elemental densities of the constituents respectively.

The nominal densities of the samples were calculated after the process of sintering was done, the volume and density of the samples were calculated.

3.4.1.2 Theoretical composite density

The inverse rule of mixtures was extended to compute the theoretical composite density (ρ_c) from the respective weight fractions (%) and theoretical densities of the matrix and reinforcing fibers, using the formula:

$$\rho_c = \frac{100}{\left(\frac{M_m}{\rho_m}\right) + \left(\frac{M_f}{\rho_f}\right)}$$

where (M_m, ρ_m) and (M_f, ρ_f) represent weight fractions (%) and density of matrix and reinforcing fibers respectively.

3.4.1.3 Density of green compacts

Green densities (ρ_g) of cold consolidated green compacts, were estimated by weighing to an accuracy of 0.1 mg using AUW120TM (Shimadzu, Japan) electronic weighing balance (120 g weighing capacity) and dimensional measurements to accuracy of 0.01 mm using MITUTOYOTM (150 mm measuring range) Digital Vernier Caliper. Measurements were repeated on at least 2 identically processed compacts, and average weight and volume values were used to report green densities.

3.4.1.4 Density of sintered compacts

Sintered densities (ρ_s) were determined by water displacement technique (Archimedes' method). Compacts were weighed in air (M_a) and distilled water (M_w) by immersion of the compacts placed on a stainless steel pan, freely suspended by a wire attachment provided at the bottom of the weighing machine (± 0.1 mg, AUW120TM, Shimadzu, Japan) in a glass beaker filled with distilled water. Water level in the beaker and depth of immersion of the compact holding pan were kept constant. Measurements were repeated on at least 2 identically processed compacts, and average weights were used to report sintered densities, by using the formula:

$$\rho_s = \frac{M_a}{M_a - M_w}$$

All densities were reported in gcm^{-3} .

3.4.1.5 Densification parameter

Densification parameter (ψ) is a dimensionless parameter, expressed as a percentage number, useful in capturing the effect of net density progression activated by sintering alone, thereby isolating the density gain achieved during prior cold consolidation. Positive values are indicative of density enhancement by sintering, negative values point towards compact expansion. It is calculated as:

$$\psi = \left(\frac{\rho_s - \rho_g}{\rho_t - \rho_g} \right)$$

where ρ_s and ρ_g are sintered and green densities respectively; theoretical density (ρ_t) corresponds to ρ_m and ρ_c for monolithic alloys and composite formulations respectively.

3.5 Microstructure

3.5.1 Sample Preparation

Sintered and secondary processed compositions were sectioned along required planes by precision cutting saw. The cut sections of the samples were hand ground on 240, 600, 800, 1200, 1500 and 2000 standard grit SiC papers (3MTM, India). Grinding lay was turned over by 90° after each paper. Care was taken to frequently dip the ground surface in water, to ensure release of SiC particles from the soft aluminum matrix. After the samples were ground on the SiC paper, manual polishing was done on open-nap (rough) billiards cloth, followed by another polishing cycle on closed-nap (fine) billiards cloth. The polished samples, were further subjected to ultrafine polishing on the Alumina cloth, while being constantly lubricated using Alumina flux.



Figure 3.9: Variable Speed Double Disc Polisher



Figure 3.10: Belt Grinder

3.5.2 Etchants and Optical Micrography

The surface of the polished samples were then cleaned using high purity ethanol and sun dried. After cleaning, for better resolution of pore size, distribution, morphology and prior particle boundaries (PPB's) of the aluminum based matrices, etchant was employed. Keller's reagent (47.5 ml Distilled Water, 2.5 ml HNO₃, 1.5 ml HCl, 1.0 ml HF) applied by a cotton swab, was most effective in revealing the desired information for Al-0.5 wt.% Mg, Al-0.5wt% Mg-1 wt.% Cu and Al-0.5 wt.% Mg-5 wt.% Cu based compositions.

Optical microscopy was performed on (equipment name) metallurgical microscopes, having 5x, 10x, 20x, 50x and 100x compound magnifications with facility for image digitization and capture.



Figure 3.11: Metallurgical Microscope

To determine the effect of reinforcement content on the different matrices, hardness of matrix, unreacted reinforcement and the reaction interface was systematically measured for the composites using FutureTech FM-700TM (Japan) Vickers microhardness tester at 50gf load for 5 seconds dwell time. Average of 3 measurements was reported for each sample in VHN. Test surfaces were parallel and polished to 2000 grit finish by using SiC grinding papers. Distance between successive indents was maintained at more than 5 times the indent diagonal.



Figure 3.12: Micro-hardness Machine

RESULTS AND DISCUSSION

CHAPTER-4

RESULTS AND DISCUSSIONS

4.1 Introduction

The alloys of various compositions of Al-Mg-Cu(Ni), synthesized through the powder metallurgy route were characterized at various stages of the experiment and their results were compared with the already published experimental results. The specimens were tested for their microstructures, micro-hardness, densities etc. These properties were checked at various stages of the powder metallurgy process, first while after sintering and at the end after the specimens were hot pressed and the difference in the properties was also discussed.

4.2 Characterization of Sintered Specimen

4.2.1 Microstructure

A section of the sintered specimens were cut out by using a cutting saw. These sections were hand ground on 240, 600, 800, 1200, 1500 and 2000 standard grit SiC papers (3MTM, India). After the samples were ground on the SiC paper, manual polishing was done on open-nap (rough) billiards cloth, followed by another polishing cycle on closed-nap (fine) billiards cloth. The polished samples, were further subjected to ultrafine polishing on the Alumina cloth, while being constantly lubricated using Alumina flux. After the cut sections were ideally polished, they were subjected to careful application of Keller's reagent (95 ml H₂O, 2.5 ml HNO₃, 1.5 ml HCl, 1.0 ml HF) by cotton swap for the observation of pore distribution, prior particle boundaries (PPB's) of the aluminum based matrices.

These etched sections were then observed via metallurgical microscope having 5x, 10x, 20x, 50x and 100x compound magnifications with facility for image digitization and capture.

4.2.1.1 Pure Al

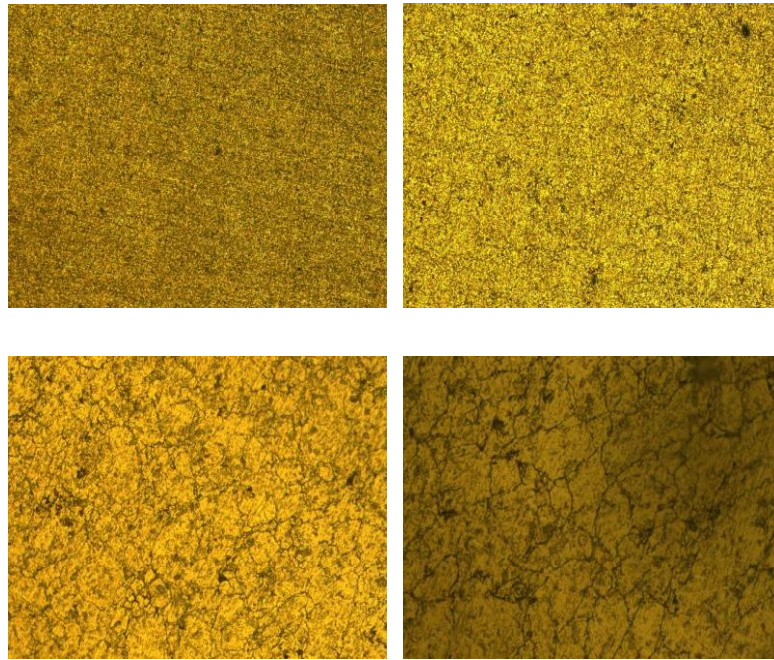


Figure 4.1(a): Microstructures of pure Al at 10x, 20x, 50x, 100x before Hot Pressing

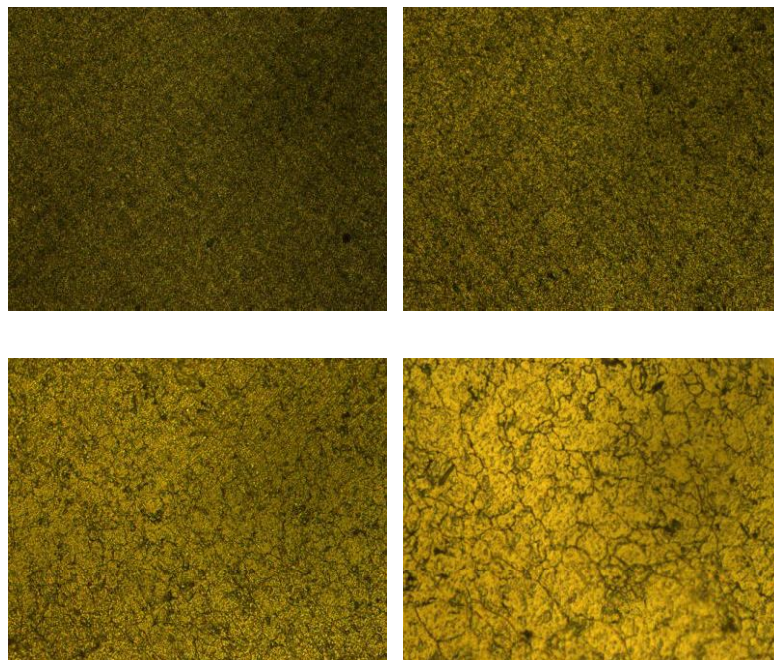


Figure 4.1(b): Microstructures of pure Al at 10x, 20x, 50x, 100x after Hot Pressing

For pure Al, we observed following microstructure as shown in Figure 4.1 (a) and Figure 4.1 (b). The figure shows a well-defined microstructure, with proper and very thin grain boundaries.

4.2.1.2 Al- Mg

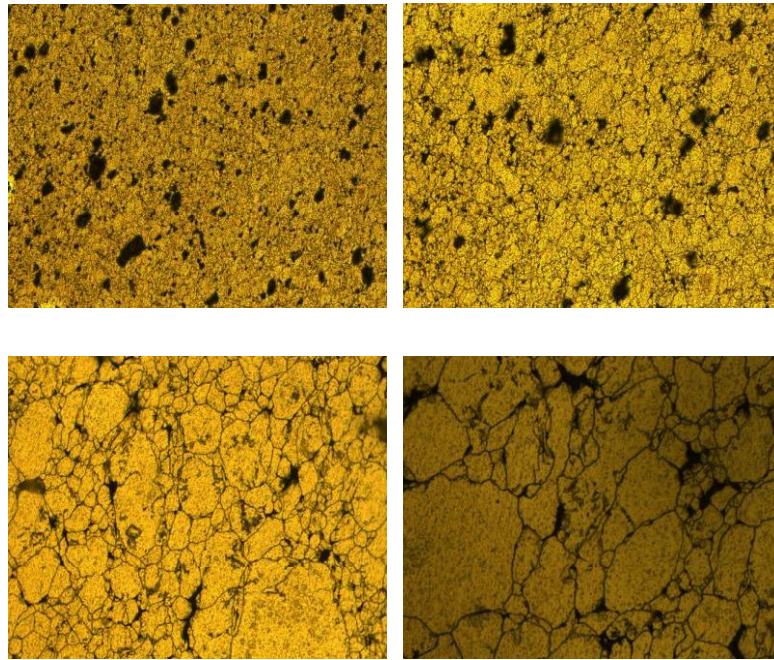


Figure 4.2(a): Microstructures of Al-Mg at 10x, 20x, 50x, 100x before Hot Pressing

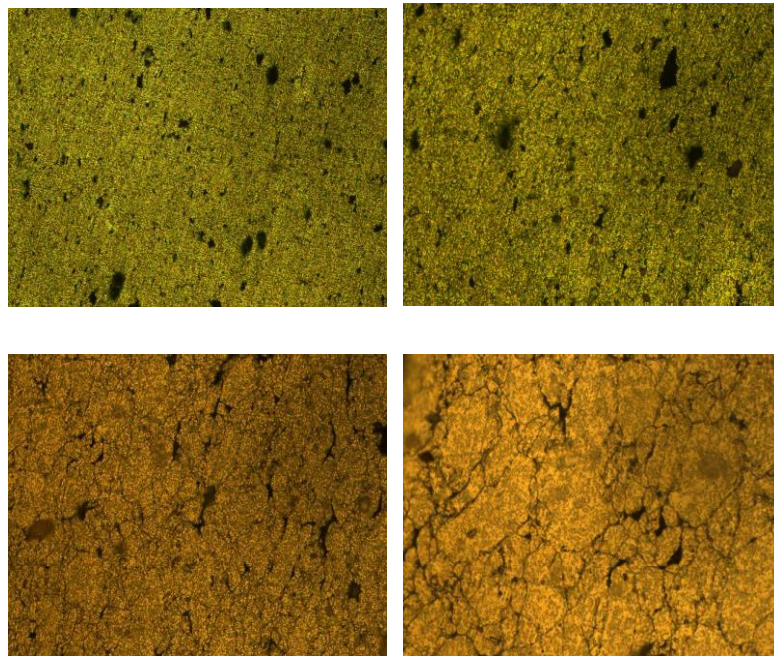


Figure 4.2(b): Microstructures of Al-Mg at 10x, 20x, 50x, 100x after Hot Pressing

In the above microstructure shown in Figure 4.2 (a) and Figure 4.2 (b), Mg reacts with aluminum in order to form spinal phases, disrupting oxide layer and aiding wetting of the sintering liquids. Magnesium content up to 0.15% causes improvements in the inter-particle bonding and densification following oxide rupture.

4.2.1.3 Al-Mg-1Cu(Ni)

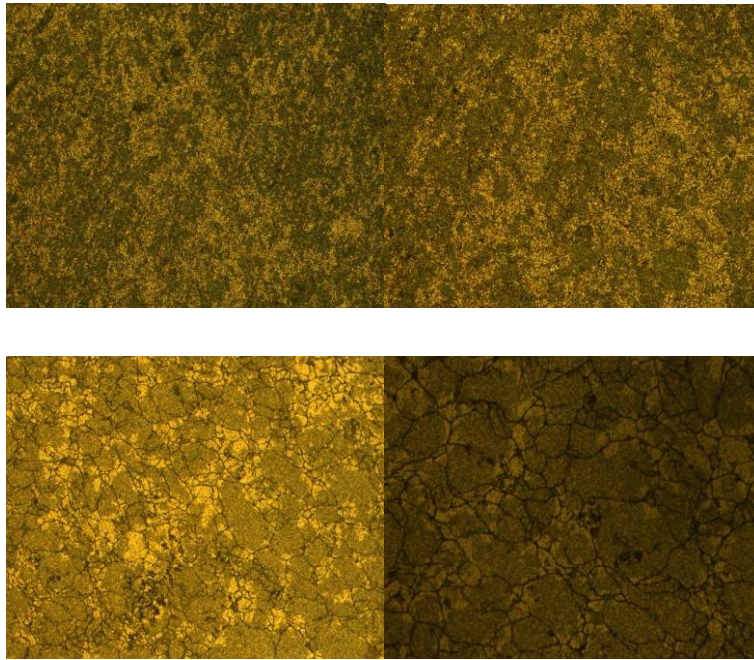


Figure 4.3(a): Microstructures of Al-Mg-1 Cu (Ni) at 10x, 20x, 50x, 100x before Hot Pressing

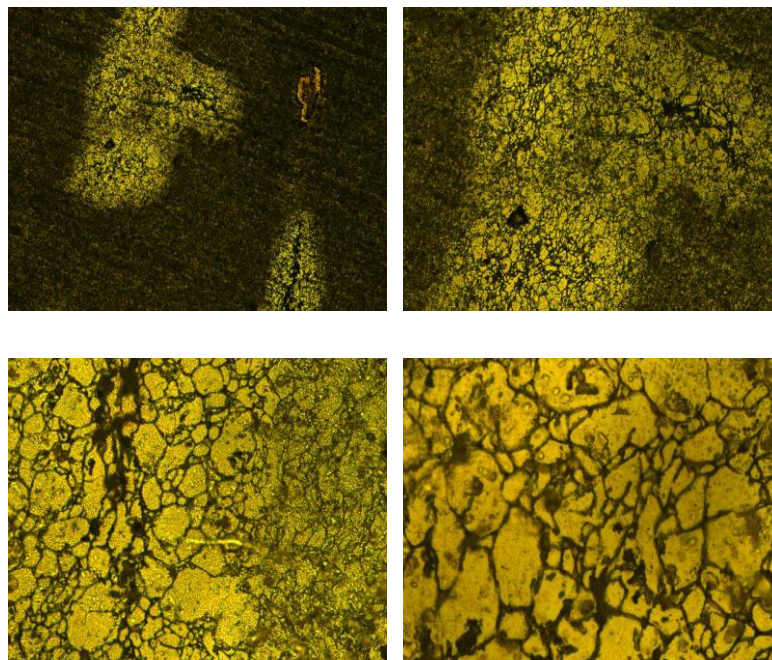


Figure 4.3(b): Microstructures of Al-Mg-1 Cu (Ni) at 10x, 20x, 50x, 100x after Hot Pressing

Microstructure of the Al-Mg-1Cu compact contains primary aluminum dendrites and copper-bearing intermetallics. Copper phases form as blocky or eutectic colonies in the inter-dendritic spaces based on cooling rate. Al_2Cu phases form simultaneously during a peritectic reaction. Porosity nucleates in the interface of dendrites and eutectic cells.

4.2.1.4 Al-Mg-5Cu (Ni)

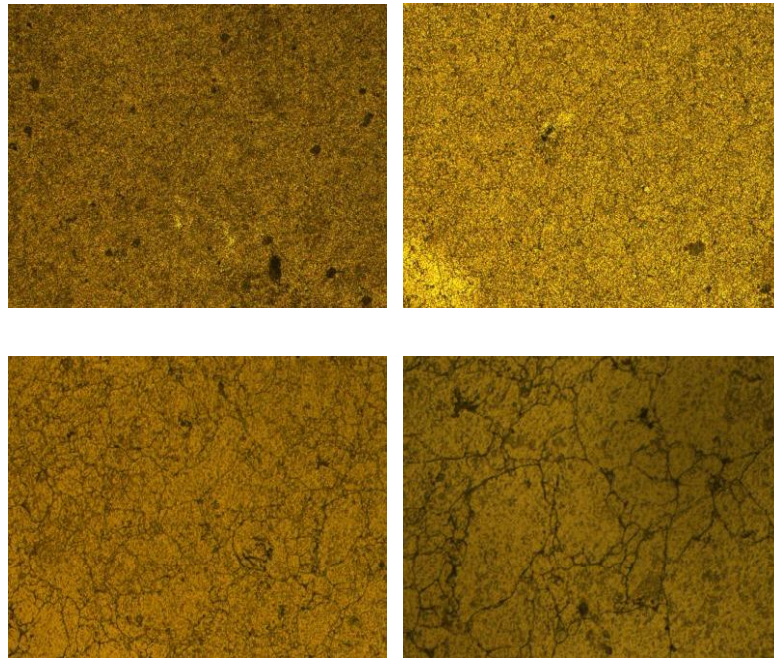


Figure 4.4(a): Microstructures of Al-Mg-5 Cu(Ni) at 10x, 20x, 50x, 100x before Hot Pressing

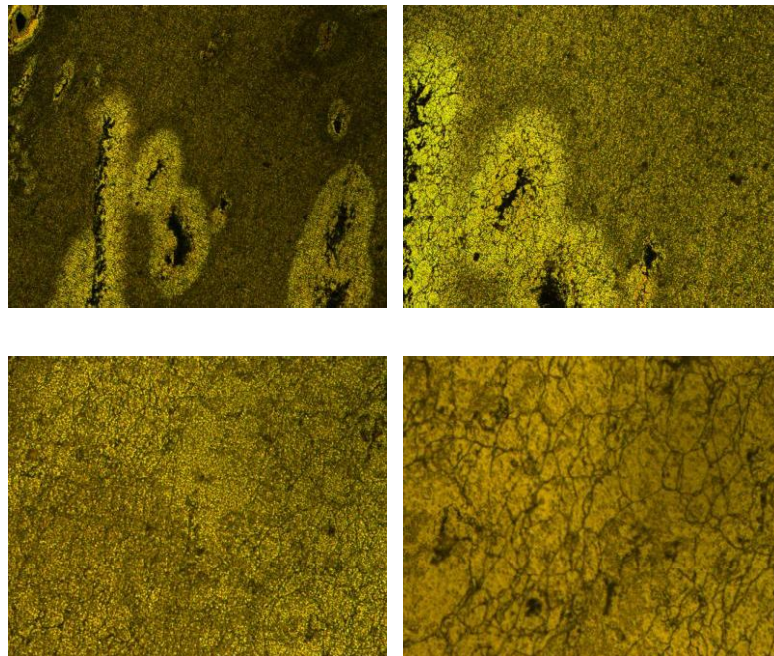


Figure 4.4(b): Microstructures of Al-Mg-5 Cu(Ni) at 10x, 20x, 50x, 100x after Hot Pressing

A very high theoretical density was achieved in Al-Mg-5Cu after sintering. A presence of some small size pores was observed. Grain boundaries of sintered Al-Mg-5Cu compact are thicker than that of sintered pure Al compact. Intermetallic phase of Al-Cu precipitates is clearly seen especially on the grain boundaries. It was supposed that precipitation of intermetallic phases on the grain boundaries and inner sides of grains stops the motion of dislocations and thus intensively strengthens the material, as this can be clearly demonstrated with the hardness discussed further.

4.2.2 Density

4.2.2.1 Theoretical Density

The dimensions of the sintered specimens were measured using high precision Vernier Calliper and the theoretical density of the sintered compacts was calculated.

For this, first the composition of the alloy in terms of parts by volume was calculated and thus, the alloy density was calculated.

Name of Component	Parts by Weight (g)	Density (g/cm ³)	Percentage by Volume
Al	99.5	2.67	99.23
Mg	0.5	0.77	0.77

Table 4.1: Composition of Al-Mg

Name of Component	Parts by Weight (g)	Density (g/cm ³)	Percentage by Volume
Al	98.505	2.67	98.93
Mg	0.5	0.77	0.76
Cu (Ni)	1	8.94	0.30

Table 4.2: Composition of Al-Mg-1Cu (Ni)

Name of Component	Parts by Weight (g)	Density (g/cm ³)	Percentage by Volume
Al	94.525	2.67	97.69
Mg	0.5	0.77	0.76
Cu (Ni)	5	8.94	1.55

Table 4.3: Composition of Al-Mg-5Cu (Ni)

On the basis of these calculations and using the rule of mixtures, the alloy densities were calculated.

$$\rho_c = \frac{100}{\left(\frac{M_m}{\rho_m}\right) + \left(\frac{M_f}{\rho_f}\right)}$$

Name of Alloy	Theoretical Density
Al-Mg	2.68
Al-Mg-1Cu(Ni)	2.71
Al-Mg-5Cu(Ni)	2.8

Table 4.4: Theoretical Densities of the sample

4.2.3 Micro Hardness

To determine the effect of reinforcement content on the different matrices, hardness of matrix, unreacted reinforcement and the reaction interface was systematically measured for the composites using FutureTech FM-700TM (Japan) Vickers micro hardness tester at 50gf load for 5 seconds dwell time. Average of 3 measurements was reported for each sample in VHN.

4.2.3.1 Before Hot Pressing

Reading	D ₁	D ₂	HV
Sample 1- Pure Al			
1.	67.99	66.84	20.40
2.	60.59	57.97	26.38
3.	53.46	60.15	28.73
			Mean: 25.17
Sample 2- Al-Mg			
1.	80.44	81.36	28.33
2.	76.42	82.00	29.55
3.	56.31	59.64	27.59
			Mean: 28.49
Sample 3- Al-Mg-1Cu(Ni)			
1.	59.96	52.54	29.36
2.	61.35	56.53	30.45
3.	58.27	53.48	28.72
			Mean: 29.51
Sample 4- Al-Mg-5Cu(Ni)			
1.	57.87	51.57	30.91
2.	58.26	54.11	29.37
3.	57.35	50.90	31.65
			Mean: 30.64

Table 4.5: Micro-hardness results (Before Hot Pressing)

4.2.3.2 After Hot Pressing

Reading	D ₁	D ₂	HV
Sample 1- Pure Al			
1.	45.80	44.47	45.51
2.	45.15	44.22	48.44
3.	41.13	46.40	48.41
			Mean: 47.45
Sample 2- Al-Mg			
1.	41.28	44.73	50.16
2.	44.24	44.99	46.58
3.	41.26	41.64	52.96
			Mean: 49.90
Sample 3- Al-Mg-1Cu(Ni)			
1.	41.52	41.00	54.46
2.	42.56	37.92	57.27
3.	47.75	40.10	48.06
			Mean: 53.26
Sample 4- Al-Mg-5Cu(Ni)			
1.	41.39	42.67	52.48
2.	43.80	41.90	48.22
3.	44.11	45.37	46.32
			Mean: 49.00

Table 4.6: Micro-hardness results (After Hot Pressing)

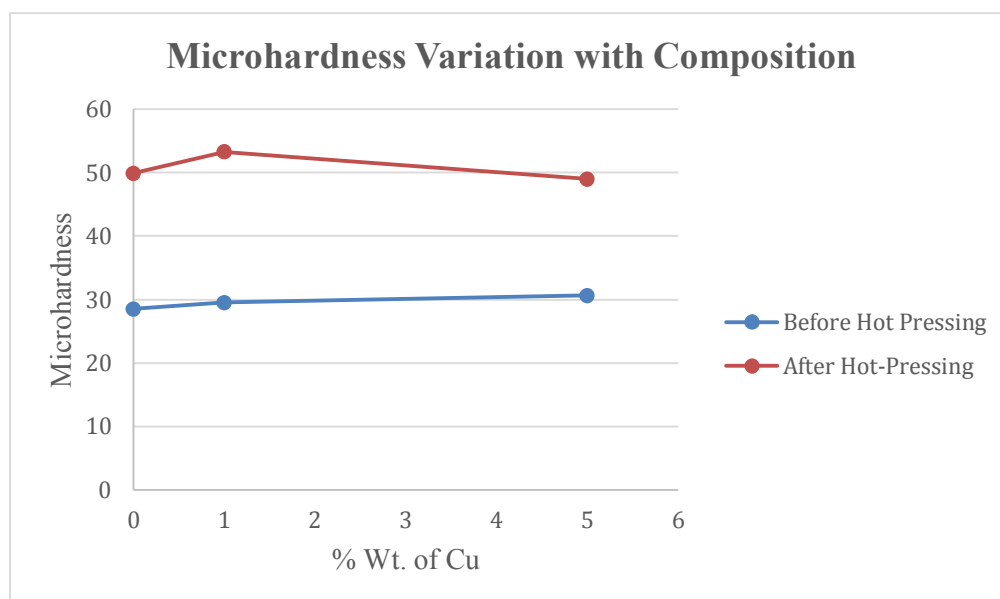


Figure 4.5: Graph showing Micro hardness with variation of Cu

Variation of microhardness with composition of Cu is the similar as with composition of Al. As the weight percentage of Cu increases the weight percentage of Al decreases linearly.

CONCLUSION

CHAPTER 5

CONCLUSION

The increasing interest in light-weight materials coupled to the need for cost-effective processing have combined to create a significant opportunity for aluminum Powder Metallurgy, particularly in the automotive industry. Aluminum Powder Metallurgy adds light-weight, high compressibility, low sintering temperatures, easy machinability and good corrosion resistance to all the advantages of conventional P/M. However, most current commercial alloys are based on standard wrought alloys, which were not designed to be sintered, and the properties are poor as a consequence. Through the work completed in this study various conclusions have been made.

- Decreasing the Mg concentration to 0.5 wt% had a detrimental effect on sintering response and mechanical properties.
- Sintering shrinkage under nitrogen occurs in three distinct stages, where the rate controlling mechanism differs in each stage.
- Through a combination of microstructural and thermal analyses it was concluded that sample was strengthened by a variety of precipitates including GP zones and η .
- Reaction between Al and Cu is detected at above 750°C to form Al_2Cu . The highest microhardness of 80MPa occurs at 700°C. The strength tends to increase with the increasing temperature due to the formation of Al_2Cu .
- The addition of copper induced a considerable age hardening effect in nickel-free alloys but this effect diminished as the nickel content increased.

REFERENCES

REFERENCES

1. Alpas, T., and Zhang, J. (1994). Effect of microstructure (particulate size and volume fraction) and counterface material on the sliding wear resistance of particulate- reinforced aluminium matrix composites. *Metallurgical and Materials Transactions A*, 25(5), 969– 983.
2. Abdel-Rahman M., and El-Sheikh, M. (1995). Workability in forging of powder metallurgy compacts. *Journal of Materials Processing Technology*, (54), 97–102.
3. Abouelmagd, G. (2004). Hot deformation and wear resistance of P/M aluminium metal matrix composites. *Journal of Materials Processing Technology*, (155-156), 1395– 1401.
4. Neubing H., Sinteraluminium – Der konsequente Weg vom Pulverprodukt zum Leichtbauteil, *Pulvermetallurgie in Wissenschaft und Praxis*, Hagen, 20(2004), 3-29.
5. Dudas, J.H., C.B. Thompson, C.B., Improved sintering procedures for aluminium P/M parts, *Aluminium Company of America Form F38-12964* (1970), 1-12
6. Schaffer G.B. and B.J. Hall, The Influence of the Atmosphere on the Sintering of Aluminium, *Metallurgical and Materials Transactions A*, 33A(2002), 3279-3284.
7. Pieczonka T., Gácsi Z., Kretz F. and Kovács J., Sintering behaviour of Al-SiC powder mixtures controlled by dilatometry, *Proc. of Euro PM2004*, compiled by H. Danninger, EPMA, Shrewsbury, UK (2004), vol. 2, 95-100.
8. Agarwala, R. C., Agarwala, V. and Garg, L.M. (1998) production of reinforced castings containing stainless steel wires in Aluminium alloy *BergUndHuttenmannischeMonatshefte*, . (143) 3 86–.89
9. Agarwala, V., Satyanarayana, K. G., and Agarwala, R. C. (1999). Studies on the development of aluminium alloy–mild steel reinforced composite. *Materials Science and Engineering: A*, 270(2), 210–218.
10. Park, B. G., Crosky, A. G., Hellier, A. K., 2001, “Material Characterization and Mechanical Properties of Al₂O₃-Al Metal Matrix Composites” *Journal of Material Science*, Vol. 36, pp. 2417 – 2426.
11. Alahelisten A., Bergman F., Olsson M. and Hogmark S. (1993). On the wear of aluminium and magnesium metal matrix composites. *Wear*, 165(April), 221–226.
12. Alsaran, A., Çelik, A., and Karakan, M. (2005). Structural, mechanical and tribological properties of duplex-treated AISI 5140 steel. *Materials Characterization*, 54(1), 85–92.
13. Arsenault, R. J. (1988). Relationship between strengthening mechanisms and fracture toughness of discontinuous SiC/Al composites. *Journal of Composites Technology and Research*, 10(4), 140– 145.
14. Asgharzadeh H., and Simchi, A. (2008). Hot deformation of PM Al6061 alloy produced by sintering and powder extrusion. *Powder Metallurgy*, 51(4), 354–360.

15. ASM International. (1990). ASM Handbook–Volume 1: Properties and Selection: Irons, Steels, and High Performance Alloys. ASM International. ASM International, Materials Park, OH, USA
16. Ibrahim, I. A., Mohamed, F. A., Lavernia, E. J., 1991, “Metal Matrix Composites” A Review Journal of Material Science, Vol.26, pp.1137 – 1157.
17. Aghajanian, M., and Rocazella, M. (1991). The fabrication of metal matrix composites by a pressureless infiltration technique. Journal of Materials Science, (26), 447–454.
18. N. Nagendra, B.S. Rao, V. Jayaram, Microstructures and properties of Al₂O₃/Al-AlN composites by pressureless infiltration of Al-alloys, Materials Science and Engineering A269 (1999) 26-37.

